Title
Ultrafast X-ray Transient Absorption Spectroscopy of Gas-Phase Photochemical Reactions: A New Universal Probe of Photoinduced Molecular Dynamics

Journal
Accounts of Chemical Research, 51(12)

ISSN
0001-4842

Authors
Bhattacherjee, Aditi
Leone, Stephen R

Publication Date
2018-12-18

DOI
10.1021/acs.accounts.8b00462

Peer reviewed

Ultrafast X-ray Transient Absorption Spectroscopy of Gas-Phase Photochemical Reactions – A New Universal Probe of Photoinduced Molecular Dynamics

Aditi Bhattacherjee[1,2] and Stephen R. Leone[1,2,3]*

[1] *Department of Chemistry, University of California, Berkeley, California 94720, USA*
[2] *Chemical Sciences Division, Lawrence Berkeley National Laboratory, Berkeley, California 94720, USA*
[3] *Department of Physics, University of California, Berkeley, California 94720, USA*

Accounts of Chemical Research

Author Information

Corresponding Author

srl@berkeley.edu

Present address

A.B. School of Chemistry, University of Bristol, Bristol BS8 1TH, United Kingdom

Notes

The authors declare no competing financial interest.

Conspectus

Time-resolved spectroscopic investigations of light-induced chemical reactions with universal detection capitalize recently on single-photon molecular probing using laser pulses in the extreme ultraviolet or X-ray regimes. Direct and simultaneous mappings of the time-evolving populations of ground-state reactants, Franck-Condon (FC) and transition state regions, excited-state intermediates and conical intersections (CI), and photoproducts in photochemical reactions utilize probe pulses that are broadband and energy-tunable. The limits on temporal resolution are set by the transit- or dwell-time of the photoexcited molecules at specific locations on the potential energy surface, typically ranging from a few femtoseconds to several hundred picoseconds.

Femtosecond high-harmonic generation (HHG) meets the stringent demands for a universal spectroscopic probe of large regions of the intramolecular phase-space in unimolecular photochemical reactions. Extreme-ultraviolet and soft X-ray pulses generated in this manner with few-femtosecond or sub-femtosecond durations have enormous bandwidths, allowing the probing of many elements simultaneously through excitation or ionization of core-electrons, creating molecular movies that shed light on entire photochemical pathways. At free electron lasers (FELs), powerful investigations are also possible, recognizing their higher flux and tunability but more limited bandwidths. Femtosecond time-resolved X-ray transient absorption spectroscopy, in particular, is a valuable universal probe of reaction pathways that maps changes via the fingerprint core-to-valence resonances. The particular power of this method over valence-ionization probes lies in its unmatched element and chemical-site specificities.

The elements carbon, nitrogen, and oxygen constitute the fundamental building blocks of life; photochemical reactions involving these elements are ubiquitous, diverse and manifold. However, table-top HHG sources in the ‘water-window’ region (280-550 eV), which encompasses the 1s-absorption edges of carbon (284 eV), nitrogen (410 eV) and oxygen (543 eV), are far from abundant or trivial. Recent breakthroughs in the laboratory have embraced this region by using long driving-wavelength optical parametric amplifiers coupled with differentially-pumped high-pressure gas source cells. This has opened avenues to study a host of photochemical reactions in organic molecules using femtosecond time-resolved transient absorption at the carbon K-edge. In this account, we summarize

recent efforts to deploy a table-top carbon K-edge source to obtain crucial chemical insights into ultrafast, ultraviolet-induced chemical reactions involving ring-opening, non-adiabatic excited-state relaxation, bond dissociation and radical formation.

The X-ray probe provides a direct spectroscopic viewport into the electronic characters and configurations of the valence electronic states through spectroscopic core-level transitions into the frontier molecular orbitals of the photoexcited molecules, laying fertile ground for the real-time mapping of the evolving valence electronic structure. The profound detail and mechanistic insights emerging from the pioneering experiments at the carbon K-edge are outlined here. Comparisons of the experimental methodology with other techniques employed to study similar reactions are drawn, where applicable and relevant. We show that femtosecond time-resolved X-ray transient absorption spectroscopy blazes a new trail in the study of non-adiabatic molecular dynamics. Despite table-top implementations being largely in their infancy, future chemical applications of the technique will set the stage for widely applicable, universal probes of photoinduced molecular dynamics with unprecedented temporal resolution.

1. Introduction

Ultraviolet-induced dynamics of organic molecules are ubiquitous – pervading across atmospheric and combustion chemistry,[1,2] to biochemical processes such as vision and photosynthesis,[3,4] to electrochemistry.[5,6] Electronic energy relaxation in molecules is invariably coupled to internuclear vibrations, often witnessing the breakdown of the Born-Oppenheimer approximation. This makes molecular photochemistry and photophysics a complex interplay of electron and nuclear dynamics. The direct, real-time visualization of the coupled electron-nuclear dynamics in photoexcited molecules is a long-standing central goal in chemistry.

The foundations of time-resolved probing of dynamics were laid down by the seminal works of Norrish and Porter, who used microsecond pulses from gas-discharge flash-lamps.[7] With the advancement of laser technology and mode-locking, it took less than forty years to improve the temporal resolution by many orders of magnitude.[8] This made it possible to probe molecular dynamics at the intrinsic timescale of molecular vibrations (femtochemistry).[9,10] Numerous time-resolved spectroscopic techniques - time-resolved electronic spectroscopy (TRES), time-resolved infrared spectroscopy (TRIR), time-resolved photoelectron spectroscopy (TRPES), etc. - have greatly contributed to the understanding of elementary chemical reactions involving bond-breaking, structural isomerizations, and non-adiabatic dynamics.[11-14]

The underlying theme of a time-resolved experiment is to first create a non-equilibrium population in an excited state using a 'pump' pulse, which starts the reaction clock with a well-defined zero-of-time.[14] Quantum mechanically, the non-equilibrium population is described as a non-stationary state, i.e., a coherent superposition of states. Its evolution is subsequently monitored using a time-delayed 'probe' pulse that projects the population onto a final state. Depending on the nature of the final state accessed, it is feasible to study the entire reaction pathway up until either equilibrium is restored (ground-state repopulation) or an irreversible electronic-nuclear dynamic process generates new photoproducts. The ultimate quest in molecular photochemistry is for universal probes of relaxation mechanisms, reaction products, intermediates, transition states, and branching fractions.

A universal probe is used to imply a widely-applicable method that is largely independent of the type of molecule, excited-state lifetimes, electronic energies, vibrational distributions, spin states

etc. Generally, core-level spectroscopy serves as a valuable probe by projecting core-electronic states onto unoccupied valence/Rydberg states.[15] The last few years have witnessed a huge upsurge in ultrafast X-ray science which has led to the commissioning/upgrading of beamlines for higher pulse-energies, shorter pulse-durations, and high repetition rates.[16] Table-top X-ray sources have flourished as well, lured by the promising advantages of the 'water-window' region – a region of the soft X-ray spectrum between 280 eV and 550 eV that spans the 1s-absorption edges of carbon, nitrogen, and oxygen. Although transient absorption spectroscopy with optical pulses is very well established, it is only recently that it has been extended to core-level X-ray probes.

Generally, transient absorption spectroscopy represents a third-order nonlinear spectroscopic technique, which employs a two-pulse pump-probe scheme – in the perturbative limit, the pump pulse represents a second-order interaction and the weak probe pulse is a first-order interaction.[17] Time-resolved X-ray absorption spectroscopy (TRXAS) experiments described here make use of a 266-nm pump pulse and a broadband, soft X-ray probe pulse. The technique has been applied to the ultrafast ring-opening of cyclohexadiene (CHD) and furfural (FFR), intersystem-crossing in acetylacetone (AcAc), and bond dissociation in dimethyl disulphide (DMDS) and chloroiodomethane (CH_2ICl), among numerous other examples currently underway in the laboratory and also performed at FELs. We show that ultrashort, broadband, energy-tunable X-ray pulses, when combined with femtosecond time-resolved transient absorption, can serve as a universal probe of photoinduced molecular dynamics.

2. High Harmonic Generation and X-ray Absorption Spectroscopy: Basic Principles

HHG is a strong-field, non-perturbative interaction of an ultrashort laser pulse with the atoms/molecules of a generation medium, which produces the odd harmonics of the driving laser frequency.[18,19] These energy-upconverted pulses can span the vacuum-ultraviolet to the hard X-ray regimes, and they have pulse durations ranging from femtoseconds to attoseconds. According to the semi-classical picture (Figure 1a), better known as the three-step model, HHG involves (1) direct or tunnel ionization of a bound, valence electron through the laser-dressed Coulomb potential barrier, (2) propagation of the free electron in the laser field and (3) recombination of the returning electron with the parent ion in the second half of the optical cycle. In the time-domain, HHG occurs every half

optical cycle and the resulting pulse train produces a spectral comb structure in the frequency domain with a peak separation of twice the driving frequency (Figure 1b). The induced polarization vanishes in centrosymmetric media for even functions of the electric field, producing only odd-order harmonics. A successful quantum mechanical model within the strong-field approximation, known as the Lewenstein model, is also used to explain the general features of HHG.[18]

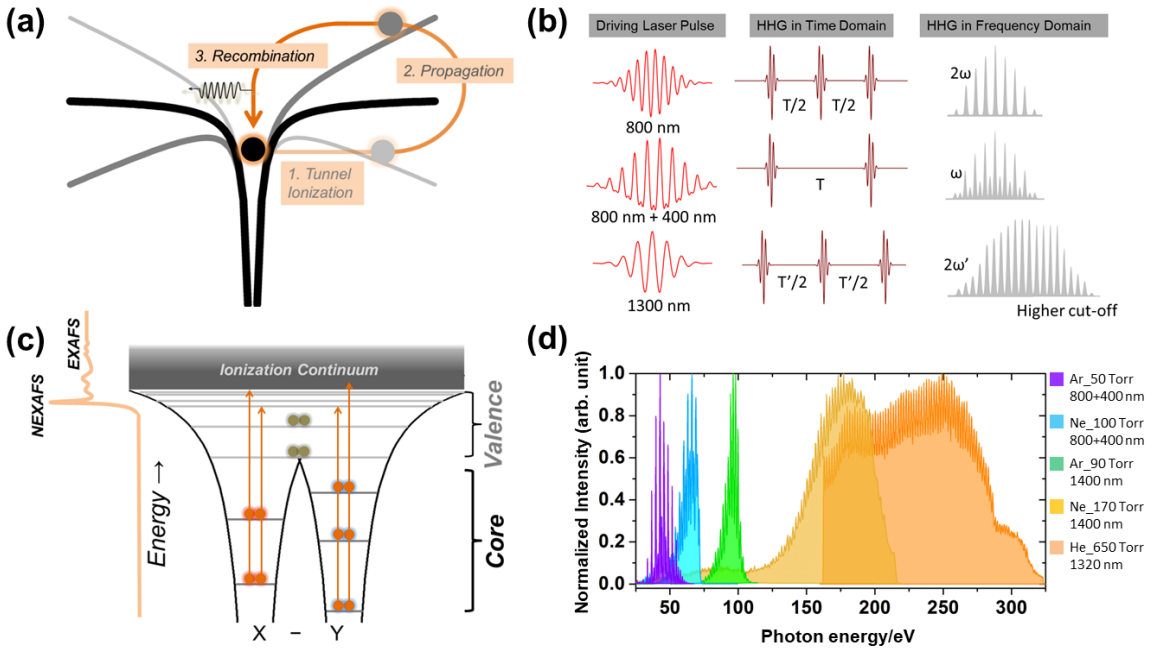

Figure 1: (a) Three-step model of HHG - coulomb potential with no external field (black line); distortions of the coulomb potential (grey) by the laser-field launches a free electron by tunnel ionization, which may subsequently recombine with the parent ion, emitting a high-energy photon (b) Schematic representations of HHG driving-laser pulses and the HHG process in time and frequency domains. (c) A representative X-ray absorption spectrum of a diatomic molecule (X-Y) shows the near-edge and extended X-ray absorption fine structures (NEXAFS/EXAFS). (d) Broadband, energy-tunable extreme-ultraviolet and soft X-ray pulses produced using a table-top HHG source in Berkeley, employing different phase-matching conditions (HHG target-gas and driving wavelengths). Schematic representations of the experimental setup may be found in Refs. 20, 38, and 39).

The energy cut-off of the emitted harmonic field is $E_{cut\text{-}off} = I_P + 3.17U_P$ (I_P is the ionization potential and $U_P = \frac{e^2E^2}{4m\omega^2}$ is the ponderomotive energy of the electron). Thus, higher cut-off energies can be obtained by using HHG-target gases with higher I_P, light pulses with higher intensity or longer driving wavelengths. Optical parametric amplifiers are often employed as $E_{cut\text{-}off}$ scales linearly with the intensity ($\sim E^2$) but quadratically with the wavelength ($\sim 1/\omega^2$). Longer driving wavelengths have the advantage of less ionization as a low free-electron density helps retain phase matching. A

disadvantage is the sharp down-scaling ($\sim\lambda^{-(5.5,6.5)}$) of the single-atom recombination efficiency due to quantum diffusion, which leads to a drastic decrease of the flux for higher-order harmonics.

A typical X-ray absorption spectrum (XAS, Figure 1c) contains a rising absorption edge from the ionization of core electrons. The absorption edge is called K, L, M, etc. corresponding to n=1, 2, 3, etc. principal quantum number. These letters carry subscripts to denote s, p, d … electrons. (K=1s; L_1=2s, $L_{2/3}$=$2p_{1/2}$/$2p_{3/2}$; M_1=3s, $M_{2/3}$=$3p_{1/2}$/$3p_{3/2}$, $M_{4/5}$=$3d_{3/2}$/$3d_{5/2}$, etc). At the onset of the edge, the so-called 'near-edge', a number of core-to-unoccupied bound state resonances dominate the XAS. This region of the spectrum is called near-edge X-ray absorption fine-structure (NEXAFS). It directly reports on the valence electronic structure of the molecule through the nature and occupancy of the frontier molecular orbitals. The extended X-ray absorption fine-structure (EXAFS) contains oscillatory features due to the scattering of the outgoing photoelectrons from nearest neighbouring atoms. It provides molecular structure information such as bond lengths, bond angles, coordination numbers, etc. In this account, we focus on NEXAFS as a universal probe of photoinduced dynamics.

3. Ultrafast Ring-Opening in a Pure Hydrocarbon – 1,3-Cyclohexadiene (CHD)

TRXAS is remarkably sensitive to the evolving valence electronic structure in the electrocyclic ring-opening reaction of CHD to 1,3,5-hexatriene (HT) - a benchmark prototype of pericyclic reactions, one of many that led to the corroboration of the Woodward-Hoffman rules. The key reaction mechanism that controls the product stereochemistry involves conservation of orbital symmetry and a smooth evolution of the valence electronic structure from reactant to product via an intermediate excited-state 'pericyclic' minimum of mixed 2π(HOMO)/$1\pi^*$(LUMO) character. Pioneering TRXAS studies at the carbon K-edge reported the evolving valence electronic structure in CHD→HT ring opening reaction.[20]

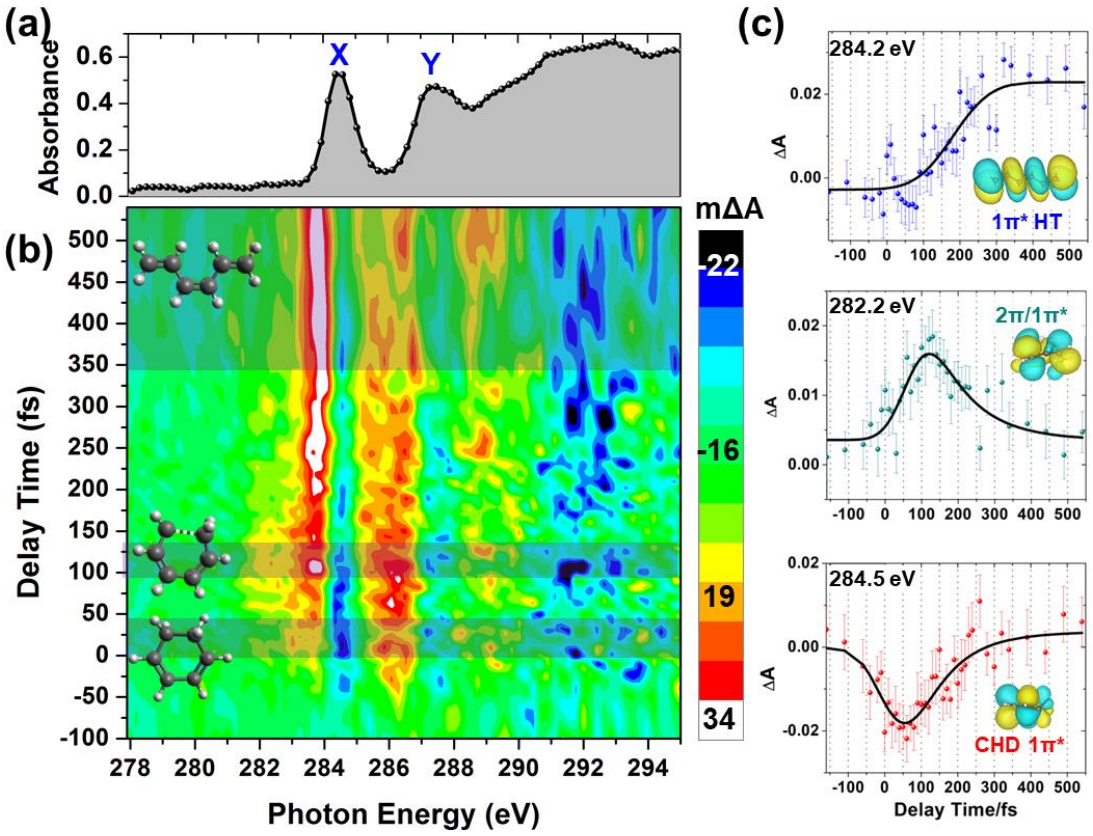

Figure 2: (a) NEXAFS spectrum of ground-state CHD (b) False-color surface map showing the changes (mΔA) in the XAS as a function of photon energy and delay time (positive delay times indicate that the soft X-ray pulse follows the UV pulse). An increase in absorbance is represented in yellow/red/white, a decrease in blue/black. Three temporal windows are indicated by the shaded regions, each representing an important step in the ring-opening reaction. (c) Temporal evolution of the peaks at 284.2 eV (final 1s1π* resonance of HT photoproduct, fit to a delayed rise of 180±20 fs), 282.2 eV (transient 1s-2π/1π* 'pericyclic minimum' resonance, fit to a delayed rise of 60 ± 20 fs and an exponential decay of 110± 60 fs), and 284.5 eV (depletion of the 1s1π* CHD resonance shows recovery due to overlapping 1s1π* resonances of both vibrationally-hot CHD and HT). The error margins in all the fitted parameters represent ±1 SE (standard error), calculated from the least-squares fitting routine. (Adapted with permission from ref. 20. Copyright 2018 American Association for the Advancement of Science)

The NEXAFS spectrum of ground-state CHD shows peaks X ($1s\rightarrow1\pi^*_{LUMO}$ transition at 284.5 eV, Figure 2a) and Y (287.3 eV from overlapping $1s\rightarrow2\pi^*_{LUMO+1}$, $1s\rightarrow\sigma^*_{C\text{-}C}$, and $1s\rightarrow\sigma^*_{C\text{-}H}$ transitions). The 266-nm-induced $S_0\rightarrow S_1(\pi\pi^*)$ excitation in CHD leaves a singly-occupied 2π-HOMO and 1π*-LUMO, immediately modifying the NEXAFS spectrum in the FC-region of excitation. Depletion of peak X and a low-energy absorbance wing (between 280.5 and 284 eV) are clearly noted in the 0-40 fs time-window (Figure 2b). The instrument response function (IRF, sub-100 fs) is not adequate to capture the fast departure from the FC region; experimental observations of the continuous shifts in the $1s\rightarrow2\pi$ and $1s\rightarrow1\pi^*$ resonances and passage through CIs entail higher

temporal resolution. Nonetheless, in the TRXAS measured between 90 and 130 fs, an intermediate resonance is clearly identified at 282.2 eV. Non-adiabatic molecular dynamics (NAMD) simulations for this time-window explain this feature as the merging of the 1s2π and 1s1π* resonances into near-degeneracy in the vicinity of the pericyclic-minimum. It constitutes a direct experimental signature of the elusive 2A-state pericyclic-minimum and represents a strong degree of mixing of the 2π and 1π* frontier molecular orbitals in this region. A measured delay of 60±20 fs between the rise of the 1s(2π/1π*) resonance (282.2 eV) and the 1s1π* ground-state depletion (284.5 eV), corresponds to the clocked-arrival time of the wavepacket from the initially excited 1B-state (S_1) to the 2A-state (S_2) minimum. This intermediate state resonance is found to decay with an exponential time-constant of 110±60 fs, representing the lifetime of the wavepacket in the 2A state before it undergoes non-adiabatic relaxation to the ground state.

At long time-delays, an increase in the width and amplitude of peak X are observed. The broadening results from the vibrational energy whereas the increase in amplitude is specific to HT because it has a higher oscillator strength for the 1s1π* resonance compared to CHD. Therefore, the observed amplitude enhancement is a clear indication of the formation of HT in substantial yield. A search for the lower limit of the HT:CHD branching ratio that reproduces the observed peak-X amplitude enhancement relative to the NEXAFS at 300 K is performed by combining the calculated CHD/HT spectra in various ratios. It gives an approximate branching ratio of 60(HT):40(CHD), in remarkable agreement with NAMD simulations (64:36). A temporal lineout of the differential absorbance at 284.2 eV is fitted to a step function with a delayed rise of 180±20 fs, which yields the ultrafast ring-opening timescale.

Several complementary time-resolved measurements used to explore CHD ring-opening dynamics are reported in the literature. Femtosecond hard X-ray scattering constitutes a direct probe of the evolving molecular structures, and it clearly reveals the evolving dynamics in real-space through mapping the nuclear motions.[21] However, scattering signals are generally broad and not able to retrieve the specific photochemical branching fractions. TRPES with various ultraviolet probe pulses have informed a detailed understanding of the complete reaction pathway in CHD with very high temporal resolution.[22] This comprehensive experiment made use of a time-sequenced progression

of Rydberg states to ionize the evolving excited-state wavepacket but this scheme is likely not easily extended to other reactions for universal applicability. TRPES of CHD with vacuum-ultraviolet pulses[23] overcomes most limitations because it constitutes a universal probe and unravels useful information about excited state (1B and 2A) lifetimes in CHD as well as HT:CHD branching fractions (70:30).

An advantage of TRPES is that there are no 'dark' states in photoionization as a range of angular momenta can be accommodated by the outgoing electron (an additional bonus is that it leaves a parent ion and charged particle detection is extremely sensitive). It must be noted that even though core-to-valence transitions in the near-edge are bound by dipole selection rules (that is, they may be allowed or forbidden), TRXAS is potentially a universal probe of photoinduced dynamics. This is because utilizing the broadband and energy-tunable HHG-based X-ray probes, it is possible to 'tune' to a favourable absorption edge of a reporter atom where a dipole-allowed core-to-valence transition is accessible (*vide infra*, Section 6). Also, at high X-ray photon energies (particularly in the hard X-ray regime), NEXAFS transitions may not be governed by dipole selection rules due to the breakdown of the electric dipole approximation at such short wavelengths.[24] Due to the relative infancy of TRXAS, there are very few photochemical problems for which both TRPES and TRXAS data exist. A direct comparison of the two techniques has been afforded by complementary theoretical simulations of non-adiabatic dynamics in ethylene.[25] It reports a high degree of simplicity (fewer core-valence transitions), sensitivity (wavepacket dynamics at CIs), and easy spectral elucidation (discrete peaks separated by few electron-volts) of TRXAS in comparison to TRPES.

4. Ultrafast Ring-Opening in an Organic Heterocycle - Furfural (FFR)

Ring-opening in CHD involves a concerted electronic rearrangement to produce an altered sequence of single and double-bonds in the product. In contrast, ring opening in many heterocyclic organic molecules proceeds via a bond fission which gives rise to an open-shell photoproduct that can subsequently isomerize (e.g. H-atom migrations) to generate a stable closed-shell species. Most spectroscopic methods are not exclusively sensitive to photochemical ring opening through the identification of the unique electronic structures of the closed-chain reactant and open-chain radical photoproduct. TRXAS offers crucial insights into the electronic structure of open-shell radicals via

fingerprint core-to-LUMO/SOMO resonances. This is evidenced in the photochemistry of FFR at 266 nm, where a unique spectrum is observed in the ring-opened carbene because the electronic structure of carbon atoms bound to the heteroatoms change significantly upon ring opening.[26]

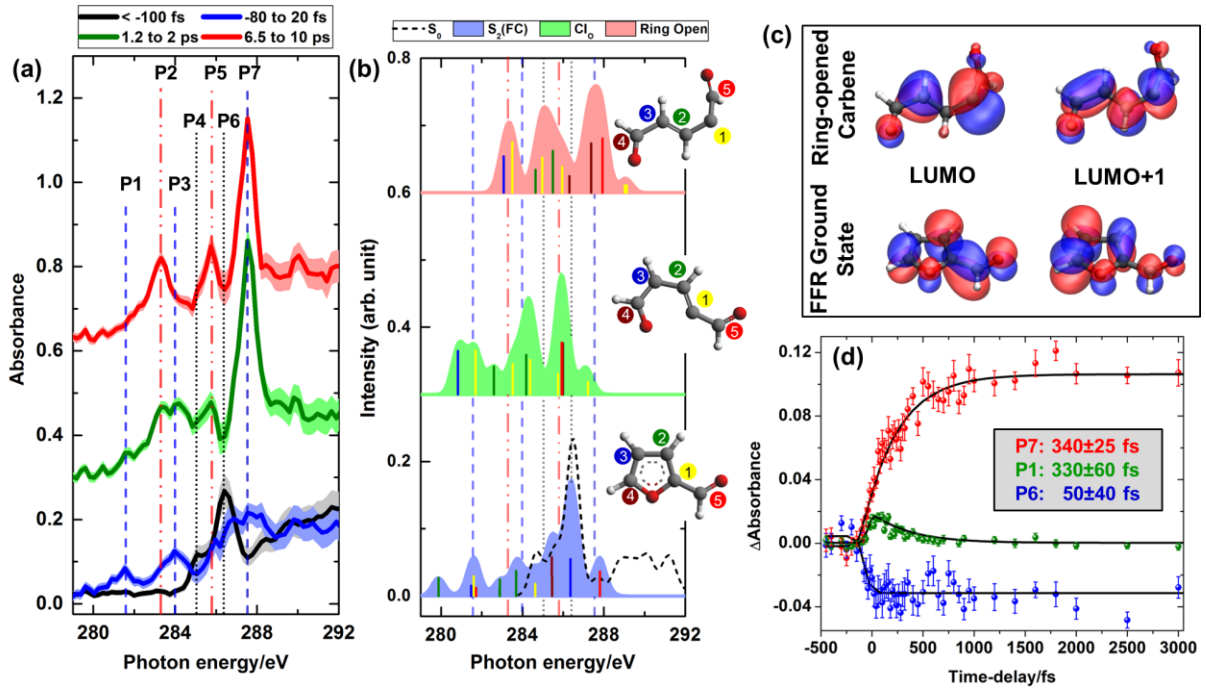

Figure 3: (a) NEXAFS spectra of photoexcited furfural derived from transient X-ray spectra measured at negative (< -100 fs, solid black line), short (-80 to 20 fs, solid blue), intermediate (1.2 to 2 ps, solid green), and long (6.5 to 10 ps, solid red) time delays. The peaks are annotated P1 through P7 in increasing order of energy. Shaded areas accompanying the solid lines represent 95% confidence interval limits. (b) Theoretical NEXAFS spectra of ground-state furfural (S_0, dashed black), FC-excited region (S_2, filled-blue), ring-opened CI (filled-green) and the ring-open carbene photoproduct (filled-red), obtained by a convolution of the underlying, color-coded stick spectra. (c) LUMO and LUMO+1 orbitals of ground-state FFR and the ring-opened carbene (d) Temporal evolutions of P1, P6, and P7 are characterized by exponential time-constants indicated in the inset. (Adapted with permission from ref. 26. Copyright 2018 American Chemical Society)

The ground-state NEXAFS spectrum of FFR (equivalent to black trace in Figure 3a) shows a double-peak structure (P6, 286.4 eV, and a low-energy shoulder P4, 285.1 eV), corresponding to chemically-shifted 1s→π*(LUMO) resonances. The TRXAS of FFR over representative time-windows shows distinct spectral changes from which the photochemical pathway is inferred. A $S_0 \rightarrow S_2(\pi\pi^*)$ optical excitation at 266-nm induces depletions of the ground-state 1sπ*(LUMO) core-excited resonances (P4, P6) at early times (blue, Figure 3a). These depletions occur immediately after photoexcitation (exponential rise-time of 50±40 fs, Figure 3d), and show constant amplitude up to 10 ps. New peaks identified in the blue trace at 281.6 eV (P1) and 284.0 eV (P3) are assigned to

transitions of a 1s-core electron into the hole left in the singly-occupied π-orbital (HOMO) resulting from the valence excitation of FFR. As the photochemical reaction proceeds to intermediate time-delays (> 1 ps, green), the amplitudes of P1 and P3 gradually decrease with the concomitant appearance of two new peaks, P2 (283.3 eV) and P5 (285.8 eV). At the longest measured time-delays (7-10 ps, red), only three new peaks remain at 283.3 eV (P2), 285.8 eV (P5), and 287.5 eV (P7).

Insights into the reaction pathway of photoexcited FFR are derived from NEVPT2-simulated NEXAFS spectra for representative points on the potential energy surface. The computed NEXAFS spectrum for the FC-region in the optically bright S_2 state agrees well with the observed early time-delay spectrum, in regard to the positions of P1 and P2. The positions of P2, P5, and P7 observed at the longest time delays are in excellent agreement with the computed NEXAFS (red curve, Figure 3b) of an open-chain carbene. P2 and P5 represent the chemically-shifted, core-LUMO resonances of the ring-open form, whereas P7 is a core-(LUMO+1) resonance. The position of P2 represents a fingerprint core-1s transition into a non-bonding orbital on the carbon atom (Figure 3c).

Here, TRXAS is able to directly monitor a heterocyclic ring-opening reaction and extract the relative propensities for reactive ring-opening versus non-reactive ring-closure. Kinetics of P1 (Figure 3d) reveals an exponential decay constant of 330±60 fs, which represents the excited-state lifetime. The ring opening is characterized by the exponential rise of P7, found to be 340±25 fs. Absence of recovery in the ground-state depletion up to the longest timescales measured (~10 ps) indicates that non-reactive internal conversion to the ground-state does not occur or is a minor channel (< 10%). In contrast, mass-gated photoionization probes are not sensitive to differentiating between structural isomers. TRXAS of FFR lays an initial groundwork for the application of X-ray core-level spectroscopy to a broad, general class of ring-opening photochemical reactions in organic heterocycles.

In the future, EXAFS studies will also be valuable for determining changes in the nuclear structure and will significantly advance the capabilities of table-top sources at the carbon K-edge. Time-resolved X-ray scattering[21,27] and Coulomb explosion imaging[28,29] are also powerful complementary methods of imaging the evolving molecular structure in photochemical reactions. A combination of these methods can potentially unravel the relative contributions of the ring-puckering

and ring-opening pathways in the photochemistry of five-membered heterocyclic rings. An increase in the temporal resolution via pump (266 nm) pulse compression and using isolated attosecond pulses at the carbon K-edge[30,31] will open exciting new possibilities for probing wavepacket dynamics at CIs.[32] With improvement in the flux of the carbon K-edge probe and the realization of a broadband, energy-tunable 'water-window' high-harmonic source, complementary studies at multiple absorption edges will enable the quantitative estimation of branching ratios and multi-channel quantum yields in photoinduced chemical reactions.

5. Ultrafast Non-adiabatic Dynamics - Internal Conversion (IC) in Thymine and Intersystem Crossing (ISC) in Acetylacetone, AcAc

IC and ISC are two prominent electronic relaxation pathways that critically govern the final outcomes of photoinduced reactions. If the non-adiabatic population transfer involves states of distinct electronic character, TRXAS can be a very valuable probe. For example, 266-nm photoinduced dynamics in the nucleobase thymine directly populates an $S_2(\pi\pi^*)$ state from which IC to $S_1(n\pi^*)$ occurs. This leads to a build-up of electron density from the delocalized π-bonding orbital to the localized non-bonding orbital of the heteroatom, evidenced by a new 1s(O)→*n*(O) transition at the oxygen K-edge (TRXAS experiment, LINAC light source).[33] Specifically, a time-delayed peak appears at 526.4 eV, which is red-shifted from the 1s(O)π* ground-state thymine resonances (531.4/532.2 eV). This peak arises from a 1s(O)→*n*(O) transition in the *n*π* state. Since the optical excitation is of ππ* nature, the delayed rise (60±30 fs) of this peak is a direct measure of the IC (ππ*→*n*π*) timescale.

We now turn to a general class of unsaturated carbonyl compounds (α,β-enones), of which AcAc is a prominent example. The high spin-orbit couplings in this class of molecules make them particularly prone to ISC from the singlet to the triplet manifold. At 266 nm, AcAc is known to eventually undergo a hydroxyl radical elimination reaction (~250 ps). The reaction pathway is theoretically shown to involve up to four excited-states - two singlets (S_2, ππ* and S_1, *n*π*) and two triplets (T_2, *n*π* and T_1, ππ*). The role of the triplet state in AcAc photochemistry has evaded experimental detection. TRXAS of AcAc show remarkable sensitivity to ISC and reveal its timescale to be much faster than previously thought.[34]

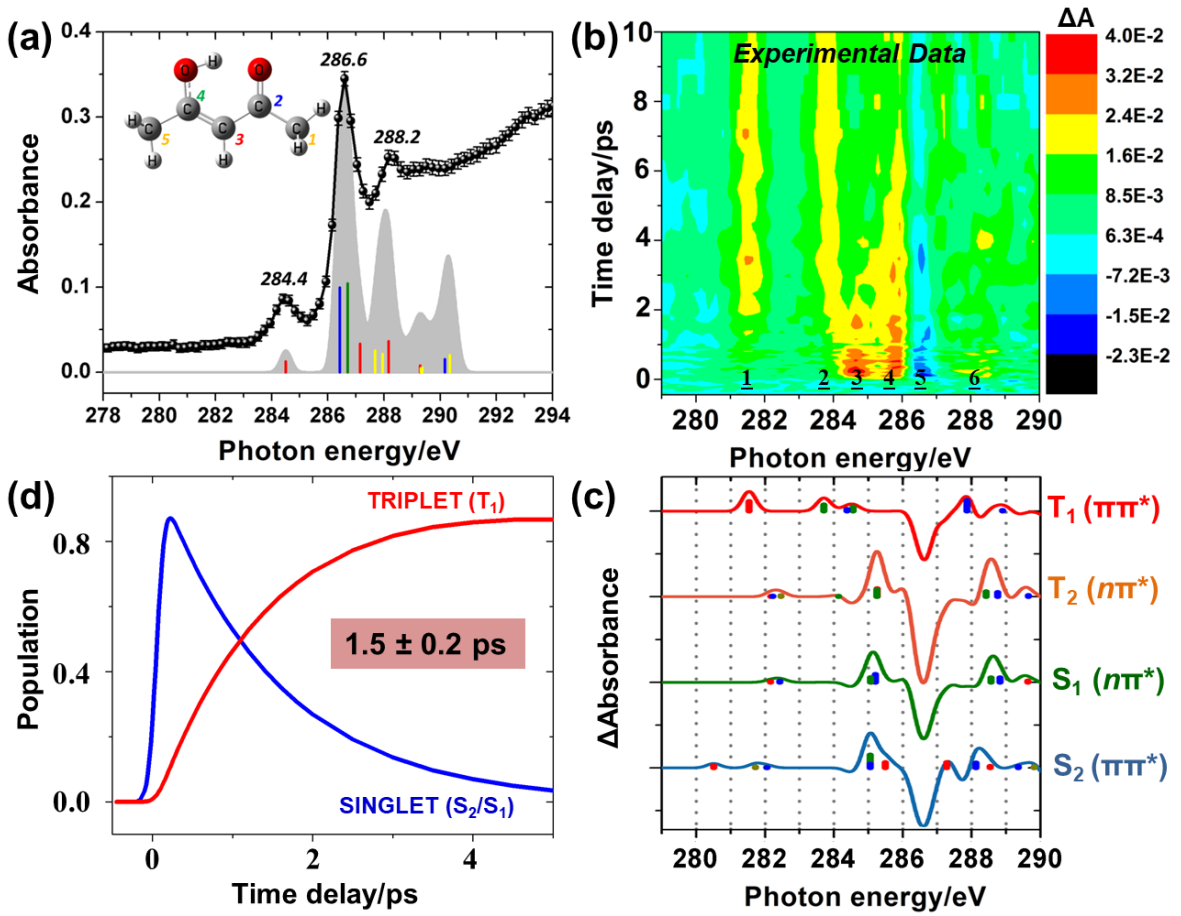

Figure 4: (a) NEXAFS spectrum of AcAc in the S_0 state (solid black line, error bars denote 95% confidence interval limits). A convolution (filled-gray) of the color-coded TDDFT stick spectrum of AcAc is shown for comparison (b) Two-dimensional contour map of the experimentally measured 266 nm-induced excited-state dynamics in AcAc shows six peaks (labelled 1−6). The color key on the right provides the scale for the measured differential absorption (ΔA). (c) Computed (TDDFT) soft X-ray differential absorption spectra of the excited electronic states. (d) A global fit of the experimental data provides an ISC time-constant of 1.5±0.2 ps. (Adapted with permission from ref. 34. Copyright 2018 American Chemical Society)

The ground-state NEXAFS of AcAc (Figure 4a) shows two chemically-shifted 1s→π*(LUMO) resonances at 284.4 eV and 286.6 eV (a third peak at 288.2 eV consists of overlapping 1s-core electronic transitions into higher-lying valence orbitals). TRXAS at the carbon K-edge (Figure 4b) maps the evolution in the peaks observed at the near-edge and offers a means to elucidate the photochemical reaction pathway. Immediately upon photoexcitation (S_0→S_2 at 266 nm), a depletion of the 1sπ* ground-state resonance (286.6 eV, peak 5) is noted alongside the appearance of three new peaks at 284.7 eV (peak 3), 285.9 eV (peak 4), and 288.4 eV (peak 6) due to excited-state absorption. All four peaks (3-6) are observed to gradually decay as new peaks appear at 281.4 eV (peak 1) and 283.8 eV (peak 2). The decay of peak 3 and the concomitant appearance of a lower-

energy peak 2 manifests as a red-shift in the spectrum in the 1-2 ps time-window. This timeframe also marks the onset of peak 1, and these two features together constitute real-time observation of ISC in AcAc, corroborated by time-dependent DFT calculations (Figure 4c). A global fit using a two-state sequential model retrieves an ultrafast ISC timescale of 1.5±0.2 ps (Figure 4d) in AcAc. It must be noted that an $S_1(n\pi^*)\rightarrow T_1(\pi\pi^*)$ ISC pathway is allowed by El-Sayed's rules but forbidden to $T_2(n\pi^*)$. The initial IC step is better suited to experimental detection at the oxygen K-edge as the S_1 state has $n\pi^*$ character. Nonetheless, the experiments suggest that the $S_2\rightarrow S_1$ IC likely occurs within the IRF (sub-100 fs).

The photoinduced dynamics of AcAc is also recently reported using TRPES with a universal ionization source at a seeded FEL (FERMI).[35] A recent breakthrough in FERMI, implementing control over the pulse energy jitter, enabled this study. Using pulses with sub-50 fs time resolution, the crucial steps in the evolution of the wavepacket were revealed and found to be consistent with the TRXAS experiments; namely an ultrafast IC to S_1 (~50 fs), complete transfer to S_1 (~ 500 fs) and ISC to T_1 (~3 ps). Ongoing developments and advancements in the generation of bright X-ray pulses at higher repetition rates and shorter pulse durations in FELs will enable routine investigations of complex photochemical reactions. Nonetheless, a table-top HHG source presents an attractive route for laboratory-based measurements of diverse photochemical reactions, with a large degree of tunability and control over the experimental conditions for systematic characterizations.

6. Ultrafast bond dissociation and radical formation – Dimethyl disulfide (DMDS) and CH_2ICl

Broadband X-ray pulses produced by an HHG source are particularly well-suited for TRXAS exploiting multiple functional groups or chemical sites. This is demonstrated in the 266 nm-photodissociation of DMDS, studied simultaneously at the sulfur $L_{1,2,3}$ edges and the carbon K-edge on our table-top source.[36] An $S_0\rightarrow S_1(n\sigma^*)$ excitation in DMDS at 266 nm can lead to a C-S or an S-S bond dissociation to produce methyl ($CH_3\cdot$+CH_3SS) or methylthiyl ($CH_3S\cdot$) radicals. TRXAS of photoexcited DMDS reveals an ultrafast S-S bond fission to form methylthiyl radicals.[36] Similarly, a C-I bond photodissociation of CH_2ICl at 266 nm ($S_0\rightarrow S_1$) allows the characterization of the CH_2Cl radical at both the chlorine $L_{2,3}$- and carbon K-edges.[37]

The NEXAFS of DMDS (Figure 5a) shows a very rich spectrum at the sulfur $L_{2,3}$ edge and somewhat simpler spectra at the sulfur-L_1 and carbon-K edges. This is because of the spin-orbit splitting at the sulfur $L_{2,3}$ edge; the peaks in this region, which correspond to the excitation of 2p electrons into σ*(S-S) or σ*(C-S) orbitals, are split by the sulfur $2p_{1/2}/2p_{3/2}$ energy difference (1.6 eV). TRXAS shows the measured $2p^{-1}$σ*(S-S) resonances that deplete immediately after photoexcitation, indicating a fast S-S bond dissociation. A core(2s)-3p(SOMO) resonance of methylthiyl radical is clearly identified at the sulfur L_1-edge at 223.0 eV and rises on a 120±30 fs timescale. The spectra measured at the carbon K-edge are also consistent with the formation of $CH_3S\cdot$ and provide a limit (~30%) for a secondary channel involving the methyl radical.

In a similar experiment on CH_2ICl photodissociation (Figure 5b), the electronic structure of the $\cdot CH_2Cl$ radical is characterized both at the carbon and chlorine edges and shows a sub-100 fs rise. An improved temporal resolution will provide access to the transition-state region and conical intersections in fast dissociation reactions. For example, femtosecond extreme-ultraviolet transient absorption spectroscopy with the same HHG set-up has been used to identify transients in the A-band photodissociation of methyl iodide and allyl iodide at the Iodine $N_{4/5}$ edge (45-50 eV), representing 4d→n and 4d→σ* core-to-valence transitions arising from the valence-excited states.[38,39] The ability of TRXAS to probe a photochemical reaction at the absorption edges of two or more constituent atoms illustrates the universality and general applicability of the method.

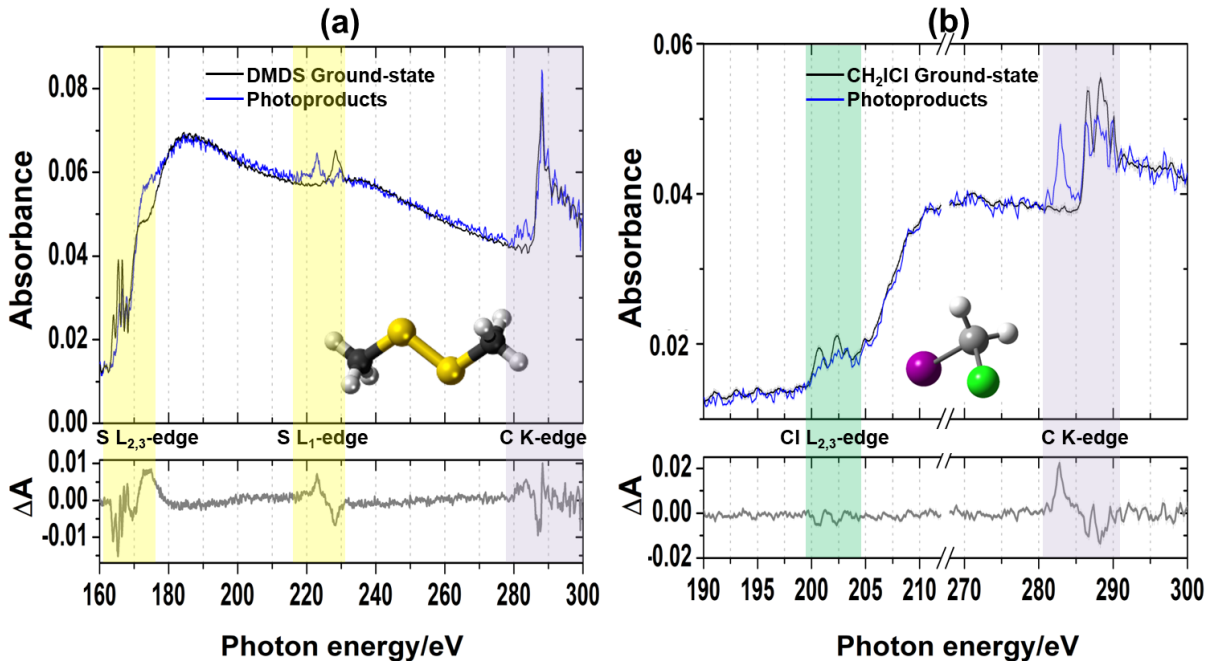

Figure 5: (a, top) XAS of ground-state DMDS (black) and photoexcitation products (blue); (bottom) differential XAS (pump-on minus pump-off) of DMDS at long time-delays (300-2000 fs). Shaded areas from left to right indicate the sulfur $L_{2,3}$ edge (yellow), sulfur L_1-edge (yellow), and the carbon K-edge (gray). (Adapted from ref. 36) (b, top) XAS of ground-state CH_2ICl (black) and $\cdot CH_2Cl$ (blue) at long delays; (bottom) differential XAS of CH_2ICl at long delays (400-1000 fs). Shaded areas denote the chlorine $L_{2,3}$ edge (green) and the carbon K-edge (gray). (Adapted with permission from ref. 37. Copyright 2018 American Chemical Society)

7. Conclusion

Recent chemical applications of femtosecond transient absorption spectroscopy at the carbon K-edge break new ground in the study of organic molecular photochemistry using a table-top HHG source. Direct probing of the constituent atoms makes the technique universally applicable to organic molecules, in pure hydrocarbons and heteronuclear compounds. The unique sensitivity of the technique to the evolving valence-electronic structure is revealed through ultrafast ring-opening reactions, non-adiabatic reaction pathways, and bond dissociations. The localized nature of the probe, coupled with the femtosecond-to-attosecond pulse durations, means that complex photoinduced dynamics will become viable in the near future. The implications are profound, impactful, and far-reaching – from direct visualizations of the ultrafast dynamics at conical intersections to ultrafast charge migrations and orbital renormalizations following electronic excitation or ionization. Access to multiple absorption edges, encompassing but not necessarily restricted to the water-window region,

will inform our understanding of the elementary steps in chemical reactions, bringing significant rewards to the fields of experimental photochemistry and photobiology.

Biographical Information

Aditi Bhattacherjee is a post-doctoral researcher with research interests in non-linear spectroscopies in the optical, infrared and X-ray regimes.

Stephen R. Leone is a Professor of Chemistry and Physics (University of California, Berkeley). He is John R. Thomas Endowed Chair in Physical Chemistry, Member of the National Academy of Sciences, and recipient of the Ahmed Zewail Award.

Acknowledgements

This research work was supported by the U.S. Department of Energy, Office of Science, Office of Basic Energy Sciences (Contract No. DE-AC02-05CH11231), the gas phase chemical physics program through the Chemical Sciences Division of Lawrence Berkeley National Laboratory. The apparatus was partially funded by a NSF ERC, EUV Science and Technology, under a previously completed grant (No. EEC-0310717). Additional support is provided by the National Science Foundation (No. 1660417) and the U. S. Army Research Office (W911NF-14-1-0383).

A.B. and S.R.L. would like to thank colleagues - Dr. Attar, Dr. Schnorr, Ms. Yang, and Ms. Xue – and collaborators – Dr. Oesterling, Dr. Pemmaraju, Dr. Closser, Dr. Delcey, Ms. Oosterbaan, Prof. Prendergast, Dr. Gessner, Prof. Neumark, Prof. Head-Gordon, Prof. Stanton, and Prof. de Vivie-Riedle.

References

(1) George, C.; Ammann, M.; D'Anna, B.; Donaldson, D. J.; Nizkorodov, S. A. Heterogeneous Photochemistry in the Atmosphere. *Chem Rev* **2015**, *115*, 4218-4258.

(2) Oberg, K. I. Photochemistry and Astrochemistry: Photochemical Pathways to Interstellar Complex Organic Molecules. *Chem Rev* **2016**, *116*, 9631-9663.

(3) Van der Horst, M. A.; Hellingwerf, K. J. Photoreceptor proteins, "star actors of modern times": A review of the functional dynamics in the structure of representative members of six different photoreceptor families. *Accounts Chem Res* **2004**, *37*, 13-20.

(4) Szacilowski, K.; Macyk, W.; Drzewiecka-Matuszek, A.; Brindell, M.; Stochel, G. Bioinorganic photochemistry: Frontiers and mechanisms. *Chem Rev* **2005**, *105*, 2647-2694.

(5) Nepomnyashchii, A. B.; Bard, A. J. Electrochemistry and Electrogenerated Chemiluminescence of BODIPY Dyes. *Accounts Chem Res* **2012**, *45*, 1844-1853.

(6) Oelgemoller, M. Solar Photochemical Synthesis: From the Beginnings of Organic Photochemistry to the Solar Manufacturing of Commodity Chemicals. *Chem Rev* **2016**, *116*, 9664-9682.

(7) Norrish, R. G. W.; Porter, G. Chemical Reactions Produced by Very High Light Intensities. *Nature* **1949**, *164*, 658-658.

(8) Bloembergen, N. From nanosecond to femtosecond science. *Rev Mod Phys* **1999**, *71*, S283-S287.

(9) Khundkar, L. R.; Zewail, A. H. Ultrafast Molecular Reaction Dynamics in Real-Time - Progress over a Decade. *Annu Rev Phys Chem* **1990**, *41*, 15-60.

(10) Polanyi, J. C.; Zewail, A. H. Direct Observation of the Transition-State. *Accounts Chem Res* **1995**, *28*, 119-132.

(11) Stolow, A.; Bragg, A. E.; Neumark, D. M. Femtosecond time-resolved photoelectron spectroscopy. *Chem Rev* **2004**, *104*, 1719-1757.

(12) Suzuki, T. Femtosecond time-resolved photoelectron imaging. *Annu Rev Phys Chem* **2006**, *57*, 555-592.

(13) Dereka, B.; Koch, M.; Vauthey, E. Looking at Photoinduced Charge Transfer Processes in the IR: Answers to Several Long-Standing Questions. *Accounts Chem Res* **2017**, *50*, 426-434.

(14) Berera, R.; van Grondelle, R.; Kennis, J. T. M. Ultrafast transient absorption spectroscopy: principles and application to photosynthetic systems. *Photosynth Res* **2009**, *101*, 105-118.

(15) Loh, Z. H.; Leone, S. R. Capturing Ultrafast Quantum Dynamics with Femtosecond and Attosecond X-ray Core-Level Absorption Spectroscopy. *J Phys Chem Lett* **2013**, *4*, 292-302.

(16) Young, L.; Ueda, K.; Guhr, M.; Bucksbaum, P. H.; Simon, M.; Mukamel, S.; Rohringer, N.; Prince, K. C.; Masciovecchio, C.; Meyer, M.; Rudenko, A.; Rolles, D.; Bostedt, C.; Fuchs, M.; Reis, D. A.; Santra, R.; Kapteyn, H.; Murnane, M.; Ibrahim, H.; Legare, F.; Vrakking, M.; Isinger, M.; Kroon, D.; Gisselbrecht, M.; L'Huillier, A.; Worner, H. J.; Leone, S. R. Roadmap of ultrafast x-ray atomic and molecular physics. *J Phys B-at Mol Opt* **2018**, *51*, 032003.

(17) Pollard, W. T.; Mathies, R. A. Analysis of Femtosecond Dynamic Absorption-Spectra of Nonstationary States. *Annu Rev Phys Chem* **1992**, *43*, 497-523.

(18) Winterfeldt, C.; Spielmann, C.; Gerber, G. Colloquium: Optimal control of high-harmonic generation. *Rev Mod Phys* **2008**, *80*, 117-140.

(19) Midorikawa, K. High-Order Harmonic Generation and Attosecond Science. *Jpn J Appl Phys* **2011**, *50*, 090001.

(20) Attar, A. R.; Bhattacherjee, A.; Pemmaraju, C. D.; Schnorr, K.; Closser, K. D.; Prendergast, D.; Leone, S. R. Femtosecond x-ray spectroscopy of an electrocyclic ring-opening reaction. *Science* **2017**, *356*, 54-58.

(21) Minitti, M. P.; Budarz, J. M.; Kirrander, A.; Robinson, J. S.; Ratner, D.; Lane, T. J.; Zhu, D.; Glownia, J. M.; Kozina, M.; Lemke, H. T.; Sikorski, M.; Feng, Y.; Nelson, S.; Saita, K.; Stankus, B.; Northey, T.; Hastings, J. B.; Weber, P. M. Imaging Molecular Motion: Femtosecond X-Ray Scattering of an Electrocyclic Chemical Reaction. *Phys Rev Lett* **2015**, *114*, 255501.

(22) Pemberton, C. C.; Zhang, Y.; Saita, K.; Kirrander, A.; Weber, P. M. From the (1B) Spectroscopic State to the Photochemical Product of the Ultrafast Ring-Opening of 1,3-Cyclohexadiene: A Spectral Observation of the Complete Reaction Path. *J Phys Chem A* **2015**, *119*, 8832-8845.

(23) Adachi, S.; Sato, M.; Suzuki, T. Direct Observation of Ground-State Product Formation in a 1,3-Cyclohexadiene Ring-Opening Reaction. *J Phys Chem Lett* **2015**, *6*, 343-346.

(24) Lindle, D. W.; Hemmers, O. Breakdown of the dipole approximation in soft-X-ray photoemission. *J Electron Spectrosc* **1999**, *100*, 297-311.

(25) Neville, S. P.; Averbukh, V.; Patchkovskii, S.; Ruberti, M.; Yun, R. J.; Chergui, M.; Stolow, A.; Schuurman, M. S. Beyond structure: ultrafast X-ray absorption spectroscopy as a probe of non-adiabatic wavepacket dynamics. *Faraday Discuss* **2016**, *194*, 117-145.

(26) Bhattacherjee, A.; Schnorr, K.; Oesterling, S.; Yang, Z.; Xue, T.; R., d. V.-R.; Leone, S. Photoinduced Heterocyclic Ring-Opening of Furfural: Distinct Open-Chain Product Identification by Ultrafast X-ray Transient Absorption Spectroscopy. *J Am Chem Soc* **2018**, *140*, 12538−12544.

(27) Glownia, J. M.; Natan, A.; Cryan, J. P.; Hartsock, R.; Kozina, M.; Minitti, M. P.; Nelson, S.; Robinson, J.; Sato, T.; van Driel, T.; Welch, G.; Weninger, C.; Zhu, D.; Bucksbaum, P. H. Self-Referenced Coherent Diffraction X-Ray Movie of Angstrom- and Femtosecond-Scale Atomic Motion. *Phys Rev Lett* **2016**, *117*, 153003.

(28) Legare, F.; Lee, K. F.; Bandrauk, A. D.; Villeneuve, D. M.; Corkum, P. B. Laser Coulomb explosion imaging for probing ultra-fast molecular dynamics. *J Phys B-at Mol Opt* **2006**, *39*, S503-S513.

(29) Ibrahim, H.; Wales, B.; Beaulieu, S.; Schmidt, B. E.; Thire, N.; Fowe, E. P.; Bisson, E.; Hebeisen, C. T.; Wanie, V.; Giguere, M.; Kieffer, J. C.; Spanner, M.; Bandrauk, A. D.; Sanderson, J.; Schuurman, M. S.; Legare, F. Tabletop imaging of structural evolutions in chemical reactions demonstrated for the acetylene cation. *Nat Commun* **2014**, *5*, 4422.

(30) Silva, F.; Teichmann, S. M.; Cousin, S. L.; Hemmer, M.; Biegert, J. Spatiotemporal isolation of attosecond soft X-ray pulses in the water window. *Nat Commun* **2015**, *6*, 6611.

(31) Li, J.; Ren, X. M.; Yin, Y. C.; Zhao, K.; Chew, A.; Cheng, Y.; Cunningham, E.; Wang, Y.; Hu, S. Y.; Wu, Y.; Chini, M.; Chang, Z. H. 53-attosecond X-ray pulses reach the carbon K-edge. *Nat Commun* **2017**, *8*, 186.

(32) Neville, S. P.; Chergui, M.; Stolow, A.; Schuurman, M. S. Ultrafast X-ray Spectroscopy of Conical Intersections. *Phys Rev Lett* **2018**, *120*, 243001.

(33) Wolf, T. J. A.; Myhre, R. H.; Cryan, J. P.; Coriani, S.; Squibb, R. J.; Battistoni, A.; Berrah, N.; Bostedt, C.; Bucksbaum, P.; Coslovich, G.; Feifel, R.; Gaffney, K. J.; Grilj, J.; Martinez, T. J.; Miyabe, S.; Moeller, S. P.; Mucke, M.; Natan, A.; Obaid, R.; Osipov, T.; Plekan, O.; Wang, S.; Koch, H.; Guhr, M. Probing ultrafast pi pi*/n pi* internal conversion in organic chromophores via K-edge resonant absorption. *Nat Commun* **2017**, *8*, 29.

(34) Bhattacherjee, A.; Das Pennaraju, C.; Schnorr, K.; Attar, A. R.; Leone, S. R. Ultrafast Intersystem Crossing in Acetylacetone via Femtosecond X-ray Transient Absorption at the Carbon K-Edge. *J Am Chem Soc* **2017**, *139*, 16576-16583.

(35) Squibb, R. J.; Sapunar, M.; Ponzi, A.; Richter, R.; Kivimaki, A.; Plekan, O.; Finetti, P.; Sisourat, N.; Zhaunerchyk, V.; Marchenko, T.; Journel, L.; Guillemin, R.; Cucini, R.; Coreno, M.; Grazioli, C.; Di Fraia, M.; Callegari, C.; Prince, K. C.; Decleva, P.; Simon, M.; Eland, J. H. D.; Doslic, N.; Feifel, R.; Piancastelli, M. N. Acetylacetone photodynamics at a seeded free-electron laser. *Nat Commun* **2018**, *9*, 63.

(36) Schnorr, K.; Bhattacherjee, A.; Oosterbaan, K. J.; Delcey, M.; Yang, Z.; Xue, T.; Attar, A. R.; Chatterley, A.; Head-Gordon, M.; Leone, S.; Gessner, O. Tracing the 267 nm-induced radical formation in dimethyl disulfide using time-resolved X-ray absorption spectroscopy. *In Preparation* **2018**.

(37) Yang, Z.; Schnorr, K.; Bhattacherjee, A.; Lefebvre, P.-L.; Ephstein, M.; Xue, T.; Stanton, J.; Leone, S. R. Electron Withdrawing Effects in the Photodissociation of CH2ICl to Form CH2Cl Radical, Simultaneously Viewed Through the Carbon K and Chlorine L2,3 X-ray Edges. *J Am Chem Soc* **2018**, *140*, 13360−13366.

(38) Attar, A. R.; Bhattacherjee, A.; Leone, S. R. Direct Observation of the Transition-State Region in the Photodissociation of CH3I by Femtosecond Extreme Ultraviolet Transient Absorption Spectroscopy. *J Phys Chem Lett* **2015**, *6*, 5072-5077.

(39) Bhattacherjee, A.; Attar, A. R.; Leone, S. R. Transition state region in the A-Band photodissociation of allyl iodide-A femtosecond extreme ultraviolet transient absorption study. *J Chem Phys* **2016**, *144*, 124311.

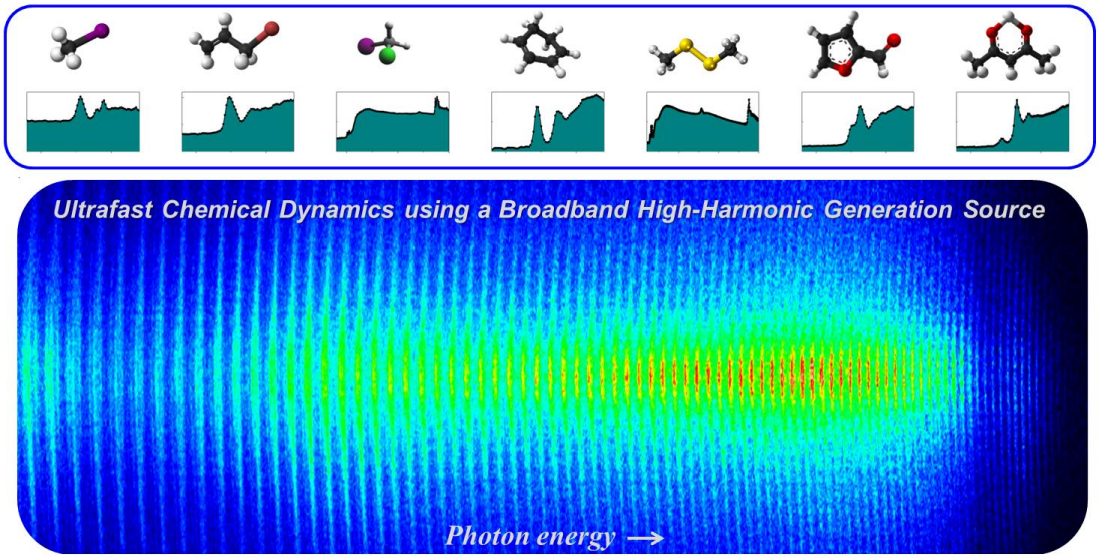
Ultrafast Chemical Dynamics using a Broadband High-Harmonic Generation Source
Photon energy

528

529